# Current control by ECCD for W7-X

Yu. Turkin, H. Maaßberg, C.D. Beidler, J. Geiger, N.B. Marushchenko

*Max-Planck-Institut für Plasmaphysik, EURATOM-Association,*

*D 17491 Greifswald, Germany*

## ABSTRACT

The magnetic configuration of the W7-X stellarator is optimized following a set of criteria including a rotational transform profile with low shear and minimized bootstrap current that must be controlled for a proper functioning of the island divertor. We study the compensation of residual bootstrap current by using electron cyclotron current drive (ECCD). The modeling shows that the loop voltage induced by ECCD leads to a redistribution of the current density with a diffusion time of about two seconds. The relaxation time of the total current is much longer, however – for W7-X plasma parameters the total toroidal current reaches steady state after several *L/R*-times requiring hundreds of seconds. In order to keep the toroidal current and its profile in the acceptable range we propose a *feed-forward* or *predictive control* method by using ECCD as actuator. The main steps are as follows: (i) calculate the bootstrap current distribution using plasma parameters measured in the *online* transport analysis, (ii) determine and apply ECCD as needed. For the current control to work properly and to avoid long relaxation times the reaction time of the control loop must be less than the current skin time.

## INTRODUCTION

One of the optimization criteria for the stellarator W7-X, is the minimization of the bootstrap current.[1] The plasma current changes the magnetic configuration, especially near the plasma edge, where X-points and islands are located. It has been shown[2] that the plasma parameters in the divertor region and the particle and energy depositions on the divertor plates depend strongly on the island geometry. An estimation of the tolerable plasma current obtained from the shift of the island structure close to the target plates shows that the plasma current should be controlled within a range of about 10 kA. The bootstrap current for high-temperatures discharges can easily exceed this value. W7-X is not equipped with an Ohmic transformer, so the only means for compensating this current is electron cyclotron current drive (ECCD) and/or neutral beam current drive (NBCD). In this report we study the compensation of residual bootstrap current by using ECCD. To model the control of the toroidal current we use a predictive 1D transport code, which is under development. In order to keep the current in an acceptable range we propose *feed-forward current control* based on online calculations of the bootstrap current and using the ECCD as actuator.

## II. METHOD

The transport code is based on a system of equations, which consists of particle and power balance equations augmented by diffusion equations for the radial electric field and for the poloidal magnetic flux:

$$
\begin{aligned}
&\frac{\partial n_e}{\partial t}+\frac{1}{V'}\frac{\partial}{\partial r}V'\Gamma_e = S_P,\\
&\frac{3}{2}\frac{\partial n_e T_e}{\partial t}+\frac{1}{V'}\frac{\partial}{\partial r}V'Q_e = P_e-\Gamma_e E_r,\\
&\frac{3}{2}\frac{\partial n_i T_i}{\partial t}+\frac{1}{V'}\frac{\partial}{\partial r}V'Q_i = P_i+z_i\Gamma_i E_r, \quad n_i=\frac{n_e}{z_i},\\
&\varepsilon_0\frac{c^2}{V_a^2}\left(1+\frac{0.7}{\iota^2}\right)\frac{\partial E_r}{\partial t}-\frac{1}{V'}\frac{\partial}{\partial r}V'D_E\left(E_r'-\frac{E_r}{r}\right)=|e|(\Gamma_e-z_i\Gamma_i),\\
&\frac{\sigma}{2\pi R_0}\frac{\partial}{\partial t}\psi_p-\frac{1}{2\pi R_0\mu_0}\frac{1}{V'}\frac{\partial}{\partial r}V'\frac{\partial}{\partial r}\psi_p = j_{bs}+j_{cd},
\end{aligned}
\qquad (1)
$$

$$
\begin{aligned}
&\Gamma_\alpha=\Gamma_\alpha^{neo}+\Gamma_\alpha^{an}, \qquad \alpha=e,i\\
&Q_\alpha=Q_\alpha^{neo}+Q_\alpha^{an}, \qquad Q_\alpha^{neo}=q_\alpha^{neo}+\Gamma_\alpha^{neo}T_\alpha,\\
&\Gamma_\alpha^{an}=-D^{an}n_\alpha', \qquad Q_\alpha^{an}=-\chi_\alpha^{an}n_\alpha T_\alpha'+\frac{3}{2}\Gamma_\alpha^{an}T_\alpha
\end{aligned}
$$

where $n_\alpha$, $T_\alpha$ and $z_\alpha$ are the density, temperature and charge number of electrons or ions, the prime denotes the derivative with respect to the effective radius $r$; $V$ is the volume enclosed in a magnetic surface with the effective radius $r$; $S_p$ is the particle source; $P_\alpha$ is the heat source/sink of species $\alpha$; $E_r$ is the ambipolar radial electric field; $D_E$ is the diffusion coefficient of the electric field, which originates from the plasma viscosity (here, for simplicity, we assume that $D_E = 0.5 m^2/s$ and does not depend on $E_r$); $\iota$ is the rotational transform; $R_0$ is the plasma major radius; $\psi_p$ is the poloidal magnetic flux related to the toroidal plasma current; $j_{bs}$ and $j_{cd}$ are the bootstrap and driven currents, respectively; $\Gamma_\alpha$ and $Q_\alpha$ are the particle and heat flux densities of species $\alpha$. The superscripts *neo* and *an* denote the neoclassical and anomalous contribution to the total fluxes. The anomalous fluxes with the diffusion coefficients $D^{an}$ and $\chi_\alpha^{an}$ are used to adjust transport at the edge area of the plasma because the neoclassical theory can not explain particle and energy loses here. In our simulations we use $1/n_e$ - dependence of anomalous diffusion coefficients with typical values chosen at the level 1-10$m^2/s$. The neoclassical heat $q_\alpha^{neo}$ and particle $\Gamma_\alpha^{neo}$ flux densities, and bootstrap current density $j_{bs}$ are given by

$$\Gamma_\alpha^{neo} = -n_\alpha\left[D_{11}^\alpha\left(\frac{n_\alpha'}{n_\alpha} - \frac{z_\alpha E_r}{T_\alpha}\right) + D_{12}^\alpha\frac{T_\alpha'}{T_\alpha}\right],$$

$$q_\alpha^{neo} = -n_\alpha T_\alpha\left[D_{21}^\alpha\left(\frac{n_\alpha'}{n_\alpha} - \frac{z_\alpha E_r}{T_\alpha}\right) + D_{22}^\alpha\frac{T_\alpha'}{T_\alpha}\right], \qquad (2)$$

$$j_{bs}^\alpha = -|ez_\alpha|\, n_\alpha\left[D_{31}^\alpha\left(\frac{n_\alpha'}{n_\alpha} - \frac{z_\alpha E_r}{T_\alpha}\right) + D_{32}^\alpha\frac{T_\alpha'}{T_\alpha}\right], \qquad j_{bs} = \sum_\alpha j_{bs}^\alpha$$

For evaluation of the transport matrix coefficients $D_{jk}^\alpha$ and the parallel conductivity $\sigma \propto D_{33}^e$ we use a database of monoenergetic coefficients precomputed by applying the DKES-code[3] and results from an international collaboration on neoclassical transport in stellarators[4].

The boundary conditions for equations (l) are the symmetry condition at the plasma center:

$$\frac{\partial n_e}{\partial r} = \frac{\partial T_e}{\partial r} = \frac{\partial T_i}{\partial r} = E_r = \frac{\partial \psi_p}{\partial r} = 0 \qquad (3)$$

The boundary conditions for the density and temperatures at the plasma edge are

$$X\big|_{r=a} = X_b, \qquad (4)$$

where $a$ is the minor plasma radius, $X$ denotes $n_e$ , $T_e$ or $T_i$ , and $X_b$ is the correspondent boundary value. The edge boundary condition for the radial electric fields is the ordinary differential equation:

$$\varepsilon_0\frac{c^2}{V_a^2}\left(1+\frac{0.7}{\iota^2}\right)\frac{\partial E_r}{\partial t}\bigg|_{r=a} = |e|\left(\Gamma_e - z_i\Gamma_i\right)\bigg|_{r=a} \qquad (5)$$

The last partial differential equation of system (1) represents the longitudinal Ohm's law; where $\psi_p$ is the self, or plasma induced, poloidal magnetic flux. Such an approach simplifies the task for finding the boundary condition – there is no need to take into account interactions of coil currents with plasma current and their mutual inductions. The stellarator W7-X is not equipped with an Ohmic transformer, so the boundary condition for the poloidal flux is the absence of an external loop voltage $\psi_p(a,t) = L\,I(a,t)$ which leads to:

$$\frac{a}{\psi_p}\frac{\partial \psi_p}{\partial r} = -\frac{R_0\mu_0}{L} \qquad (6)$$

where $I(a,t)$ is the toroidal plasma current and $L = R_0\mu_0\left(\ln\left(8R_0/a\right) - 2\right) \approx 18\mu H$ is the estimation of the W7-X plasma inductance.

## III. PLASMA RESPONSE TO CURRENT AND TIME SCALES

In the computer simulation described below, we determine the radial electric field, neoclassical fluxes, bootstrap currents, and parallel conductivity using the transport equations with a fixed density profile. During calculations we use the W7-X standard magnetic configuration with magnetic

induction of 2.5T* without self-consistent updating of the equilibrium. This makes the system (1) inexact. The reasons to use such an approximation are the following. The stellarator W7-X has been designed to have a very small bootstrap current. The absolute value of the plasma current should not exceed 10 kA to provide proper island position near the divertor plates; such a current does not change significantly the magnetic geometry. The equation for the poloidal magnetic flux has weak coupling with the other equations; the poloidal flux influences other equations only through the rotational transform and geometry changes, which should be small; but in turn this equation strongly depends on the bootstrap current and conductivity defined by densities and temperatures. These considerations provide reasonable accuracy of the system (1) for studying plasma current evolution problems described here.

Before studying the plasma response to ECCD, we equilibrate the system of equations (1) to steady state without applying ECCD. After equilibration we 'turn on' the off-axes counter-ECCD with a total value of 43kA, which is equal to the estimated bootstrap current. The prescribed current distribution $j_{eccd} \propto \exp\left(-(r-r_c)^2/w^2\right)$ is used for modeling of the ECCD. This ECCD scenario was chosen since we want to isolate and study the transient processes of a current evolution; – there is only weak coupling of the current diffusion equation with the transport.

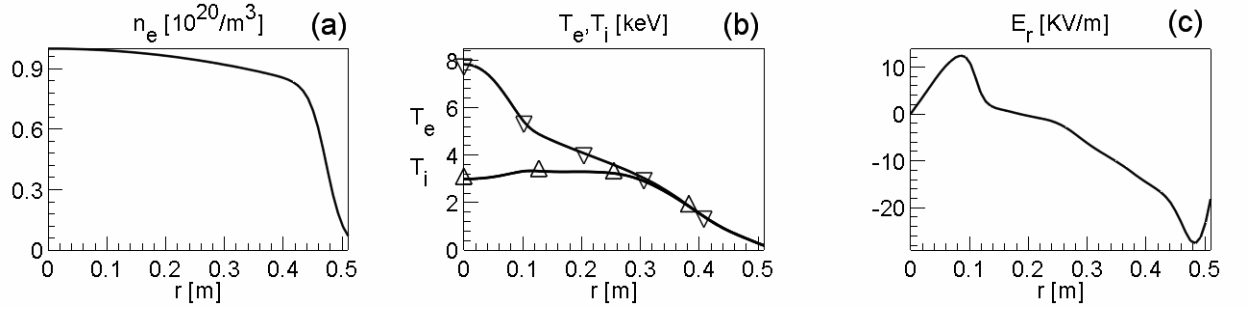


**Fig. 1.** Plasma profiles: (a) the electron density; (b) the electron (∇) and ion (Δ) temperatures; (c) the radial electric field.

In Fig. 1 the density and temperatures for the electron cyclotron resonance heating (ECRH) scenario along with the ambipolar radial electric field are shown. The electric field has a positive solution (electron root) in the central part. This behavior of the electric field is typical for such temperature profiles. The parallel conductivity, bootstrap current and counter-ECCD densities are shown in Fig. 2. After switching on the ECCD a loop voltage is induced. The radial profiles of the loop voltage are shown in Fig. 2c for several times: at 0.2sec, at 2sec, and at 25sec after applying counter-ECCD.

* corresponds to 140GHz for electron cyclotron resonance heating (ECRH) at the second harmonic of the extraordinary mode (X2-mode)

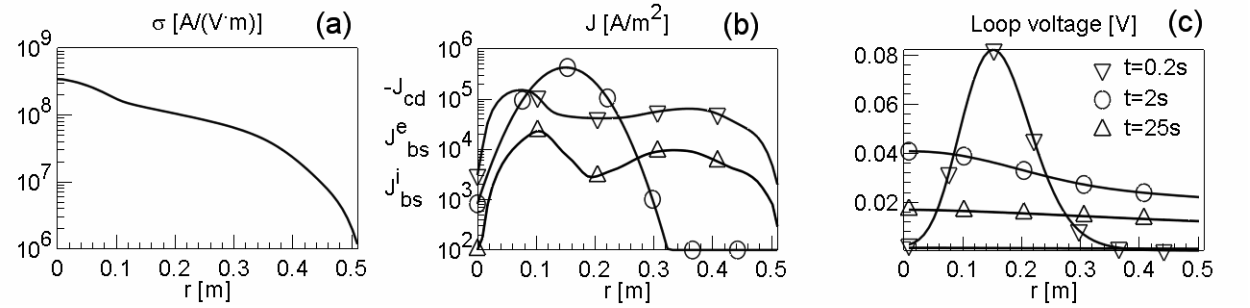


**Fig. 2**. (a) plasma conductivity; (b) the electron (∇), ion (Δ) bootstrap current densities, and ECCD (O) density; (c) time evolution of the loop voltage.

The diffusion time of the loop voltage ('skin time' – time needed for the loop voltage to reach the plasma edge) is about 2sec; the skin time can be estimated using the formula $l^2\sigma\mu_0$, where $l$ is the characteristic scale length. On this timescale, the loop voltage produces a current which considerably increases the rotational transform in the bulk plasma leaving the edge value of the rotational transform $\iota_a$ unaffected; see the curve marked by Δ in Figs. 3a and 3b.

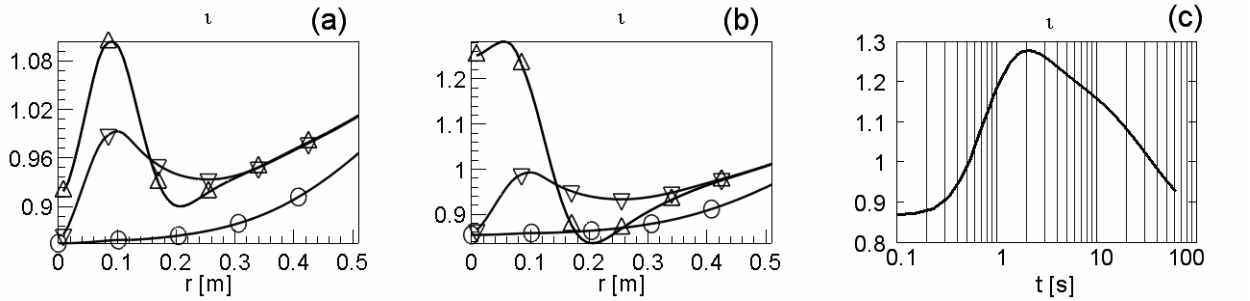


**Fig. 3**. Time evolution of the rotational transform: (a) (Δ) at 0.2 sec after applying ECCD; (b) (Δ) at 2 sec after applying ECCD; ∇ denotes the initial (without ECCD) rotational transform and O is the current-free contribution to the rotational transform; (c) time evolution of the rotational transform on axis.

For calculating the rotational transform we use the formulas:[5]

$$\iota = \frac{\mu_0 I_{tor}}{S_{11}\psi'_{tor}} - \frac{S_{12}}{S_{11}}, \quad S_{jk} = \frac{1}{4\pi^2}\int_0^{2\pi}\int_0^{2\pi}\frac{g_{jk}}{g}\sqrt{g}\; d\theta d\varphi,$$
$$I_{tor} = \int_0^r j_{tor}(x)\frac{V'(x)}{2\pi R_0}dx \qquad (7)$$

where $g_{jk}$ are the metric tensor elements, $\sqrt{g}$ is the Jacobian; $\theta$, $\varphi$ are the poloidal and toroidal angles in Boozer coordinates; $\psi'_{tor}$ is the derivative of the toroidal flux with respect to the effective radius $r$; $j_{tor}$ is the toroidal current density (the second term in the equation for the poloidal magnetic flux); $I_{tor}$ is the toroidal current; and $S_{jk}$ is the susceptance matrix. This approach allows us to

decompose the rotational transform in the current free part[†] $\iota_{CF} = -S_{12}/S_{11}$ and in the part which explicitly depends on the toroidal current and scales as $\Delta\iota \propto I_{tor}/r^2$. We also use the fact that the susceptance matrix S and the current-free contribution to the rotational transform have a weak dependence on $I_{tor}$.[5]

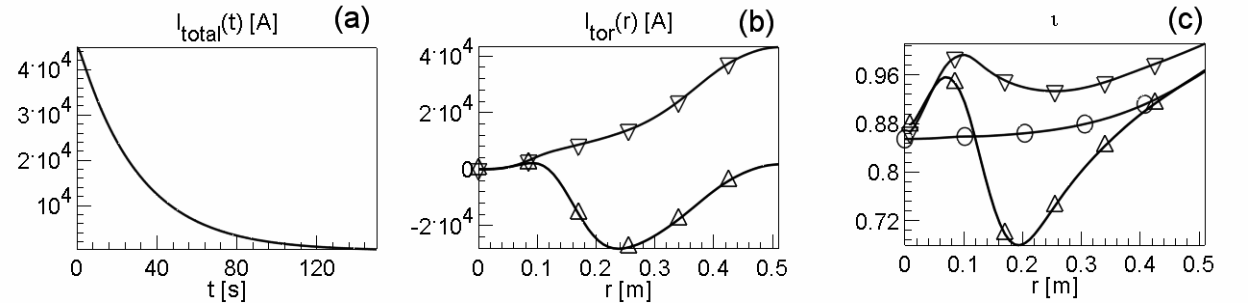


**Fig. 4**. (a) time evolution of the total current; (b) the initial (∇) and final (Δ) toroidal current distributions; (c) the initial (∇), final (Δ), and current-free (O) rotational transform.

The relaxation time of the plasma current $I_{total} = I_{tor}(a)$ is much longer than the skin time. The plasma current reaches steady state after 100 seconds with the decay time $L/R \approx 32\,\mathrm{sec}$; see Fig. 4a and also the evolution of the rotational transform in the plasma center in Fig. 3c after 2 seconds. The initial and final current distributions and associated rotational transforms are shown in Figs. 4b and 4c. The bootstrap current (curve marked by ∇ in Fig. 4b) increases the edge value of the rotational transform; $\iota_a$ going to one (∇-curve in Fig. 4c) means that the X-points and islands move inward. This represents a potential danger for the proper functioning of the island divertor used in W7-X, since the main recycling zones move away from the divertor gap. Counter-ECCD compensates the bootstrap current and decreases $\iota_a$, while in the bulk plasma the shear of the rotational transform changes sign due to localized ECCD (Δ- curve in Fig. 4c).

Let us consider the case of the on-axis counter current drive. We use the same plasma profiles and the total value of ECCD as in the previous case, which is equal to the bootstrap current. The final results of the simulation are shown in Fig. 5. On-axis localization of ECCD leads to a strong decrease of the rotational transform in the central region of the plasma, whereas the edge $\iota$-value is the same as in the case of off-axis ECCD; see Δ-marked curve in Fig. 5c. It should be noted that our computational model of a fixed equilibrium with only a small perturbation by the toroidal current is no longer valid in this case.

---

[†] here we use the terminology of Ref. 5; however the 'current free part' of the rotational transform implicitly depends on the toroidal current through flux surface averages of metric quantities, but this dependence is weak except in the case of strong on-axis ECCD ; see also Fig.6 and discussion in Ref. 5

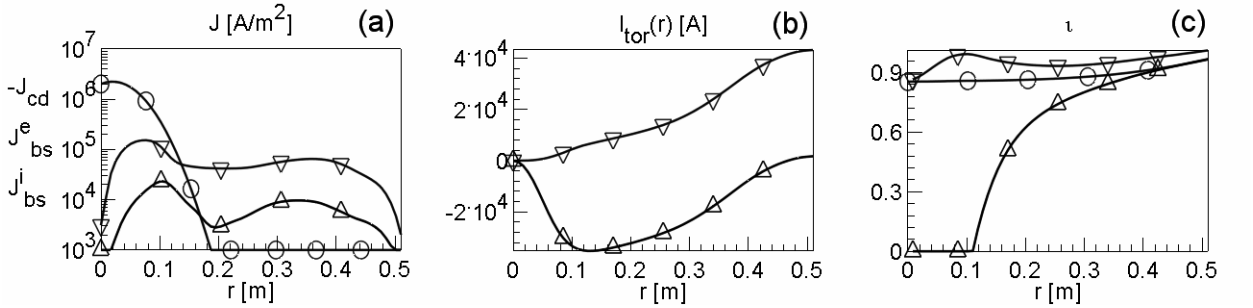


**Fig. 5**. (a) the electron (∇) and ion (Δ) bootstrap current densities, ECCD (O) density; (b) the initial (∇ ) and final (Δ) toroidal current distributions; (c) the initial (∇), final (Δ), and current-free (O) rotational transform.

It can be seen from the rotational transform expansion (7) that near the axis due to the leading dependence $\Delta\iota \propto I_{tor}/r^2$ the rotational transform changes considerably, which in turn strongly affects the equilibrium and consequently the current-free part of the rotational transform. Using the approach of Ref. 6, we set the rotational transform to zero in the central part of the plasma (Δ-curve in Fig. 5c) in order to show the tendency for the case of on-axis counter-ECCD. This part of the plasma can be considered as a region nearly without confinement due to the large deviation of particle orbits from the flux surfaces; more comprehensive analysis is needed to study this problem including MHD equilibrium calculations.[6]

## IV. CURRENT CONTROL

The magnetic configuration of the W7-X stellarator is optimized following a set of criteria listed in Ref. 1 including a flat rotational transform profile with low shear and a very small bootstrap current. To compensate the bootstrap current we need a 'control' tool that can react immediately to changes of the bootstrap current by applying counter-ECCD, i.e. the non-inductive current of the same value, but in the opposite direction. The usual feedback control scheme seems to be unfeasible because (i) there is no means to measure the bootstrap current density profile and (ii) measurements of the total current can not provide the information needed for a feedback loop due to the long *L/R*-time. In order to control and to keep the toroidal current and its shape in a tolerable range and to avoid long relaxation times we propose *feed-forward* or *predictive control* schemes using ECCD as an actuator. The steps of the method are as follows: (i) calculate the bootstrap current distribution using the measured densities and temperatures profiles in the online transport analysis and (ii) determine and apply the ECCD that is required for compensation.

For the simulation of this control algorithm, we determine the radial electric field, neoclassical fluxes, bootstrap currents, and parallel conductivity using the transport equations (1) with a fixed density profile and fixed standard magnetic configuration with magnetic induction of 2.5T. For modeling ECRH and ECCD we use prescribed profiles and the results of Ref. 7 for the ECCD efficiency. The

heating scheme is shown in Fig. 6c: **P1** is the on-axis heating source without ECCD and **P2** is the off-axis heating source which produces ECCD.

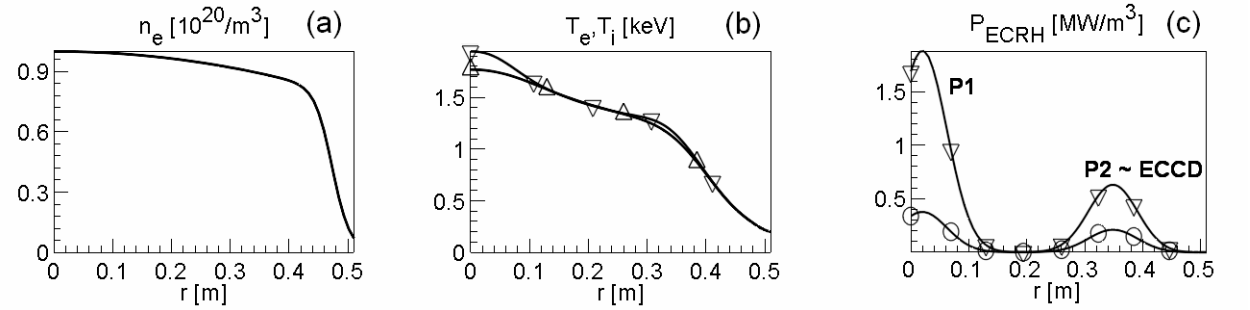


**Fig. 6**. Plasma profiles: (a) the electron density; (b) initial electron (∇) and ion (Δ) temperatures; c) initial (O) and final (∇) power deposition profiles;

For simplicity we choose fixed positions and width of both sources. Before simulation of the control algorithm, we equilibrate the system to steady state with **P1**=0.25MW and enough counter-ECCD (**P2=**1.68MW) to cancel the 7kA of bootstrap current. Corresponding initial plasma profiles and heating sources are shown in Fig. 6.

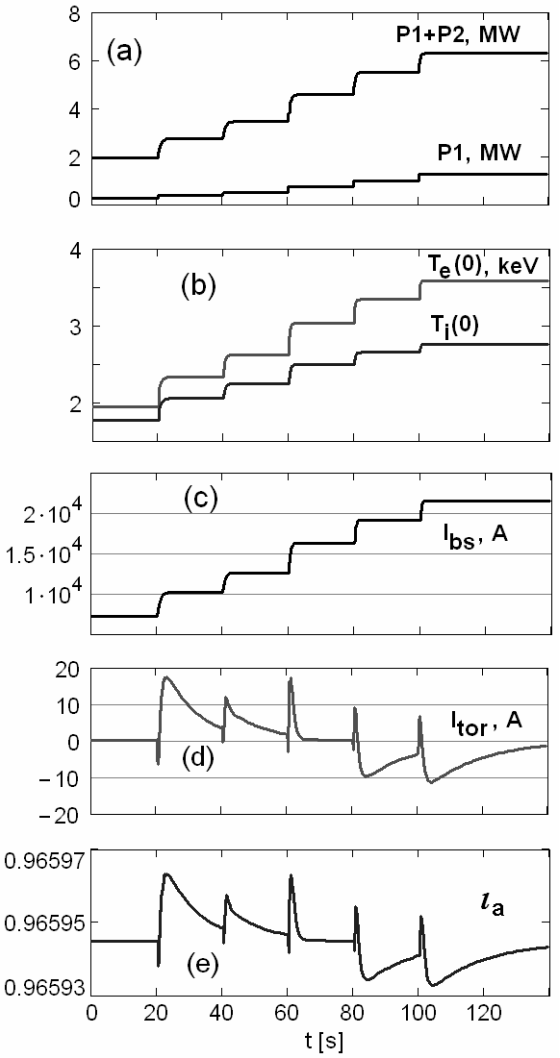


**Fig. 7**. Time traces of: (a) the heating powers, (b) the temperatures at the center, (c) the bootstrap current, (d) the total toroidal current, (e) the value of $\iota_a$ . The reaction time is 0.2 sec.

During the simulation, we increase the on-axis heating source **P1** (which has no ECCD) each 20 seconds in order to check how the control algorithm works. Increased core heating leads to an increase in the bootstrap current. According to the *feed-forward* control algorithm, the program 'measures' the total value of the bootstrap current $\mathbf{I_{bs}}$ and 'applies' the same amount of counter-ECCD $\mathbf{I_{cd}}$ by increasing the power of the heating source **P2.** The time interval between adjusting the ECCD is the reaction time of the control loop. For the current control to work properly the reaction time (in our modeling we use 0.2 and 1 second) must be less than the skin time which is about two seconds. The time traces of the total heating power, temperatures at the center, the value of $\iota_a$, the bootstrap and the total toroidal currents are shown in Fig. 7. The bootstrap current (Fig. 7c) during our computer experiment increases from 7kA to 21.5 kA owing to increased core heating **P1** (used as 'disturbing' source) and off-axis heating **P2** (used for current control). Fig. 7d and Fig. 7e show the results of the modeling with the reaction time of 0.2sec. The plasma current is less than 20A and oscillates near zero; see the $\mathbf{I_{tor}}$ - curve in Fig. 7d. The rotational transform (Fig. 7e) fluctuates near the current-free value; the changes of $\iota_a$ are less than 0.01%. Heating increases the plasma temperature and hence, the bootstrap current that must be compensated by ECCD using the same heating. Because of this "positive" feedback, according to Fig. 7a, the small increment in the core heating **P1** requires a large increase of the total heating power. Such behavior is due to our choice of the ECCD source. Here we take the ECCD proportional to the heating power **P2**. Probably, a better option is to keep the heating power fixed and adjust ECCD by changing the angle between the microwave beam and the magnetic field.

The time traces of the heating powers and currents for the time interval 19–29 sec are shown in Fig. 8. It is seen that the increase of the on-axis heating **P1** triggers the control algorithm, which produces oscillations of the non-inductive current source $\mathbf{I_{bs}} + \mathbf{I_{cd}}$ trying to keep it at the zero level (see Fig. 8c). This residual current creates poloidal flux and, as a result, an inductive current which contributes to the total current. The inductive current diffuses with the skin-time, "smoothing" the total current (compare Fig. 8c and 8d.). The changes, "accumulated" in the poloidal flux, relax with the L/R time (see the evolution of the total current after 23 sec in Fig. 8d). In this connection, the usual method of feedback control, which uses detuning of the *total plasma current* from the zero level for defining the control loop, seems to be unachievable because of the retarded response to the control action. Unlike the feedback scheme, the feed forward control algorithm proposed here "measures" the deviation of the *current source* $\mathbf{I_{bs}}+\mathbf{I_{cd}}$ from the zero level directly and takes control action over short time scales to reduce the disturbance.

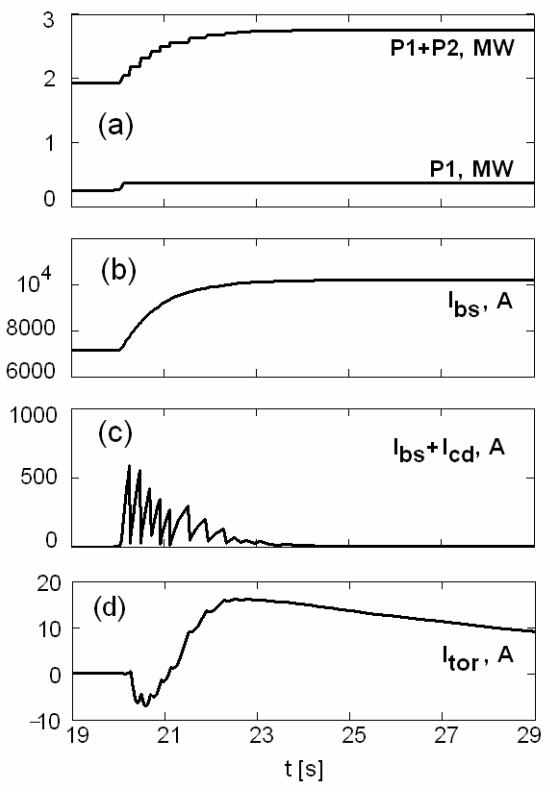


**Fig. 8**. Time traces of: (a) the heating powers, (b) the bootstrap current, (c) the sum of bootstrap current and counter-ECCD, (d) the total toroidal current. The reaction time is 0.2 sec.

The results of calculations with a 1 sec reaction time are shown in Fig. 9d and Fig. 9e. The maximum value of the total toroidal current (Fig. 9d) is about 200A. The edge rotational transform (Fig. 9e) oscillates at a level which is only 0.1% higher then the current-free value. For both values of reaction time, the control algorithm maintains a fixed edge rotational transform value.

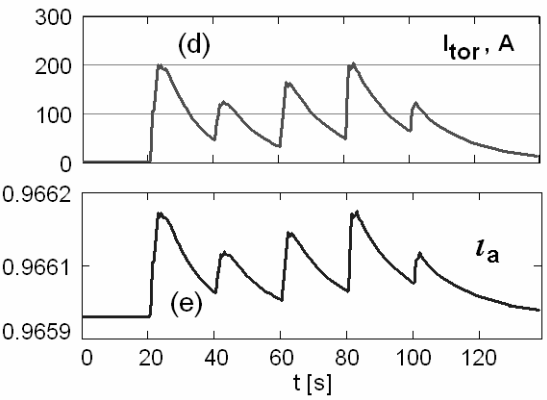


**Fig. 9**. Time traces of: (d) the total toroidal current, (e) the value of $\iota_a$. The reaction time is 1sec.

The final current distributions and associated rotational transforms are shown in Fig. 10. Without the current control the bootstrap current (see the curve marked with ∇ in Fig. 10b) would increase the edge value of the rotational transform. The counter-ECCD compensates the bootstrap current and decreases the edge value of the rotational transform, while in the bulk plasma the rotational transform ( Δ-curve in Fig. 10c) has a slightly non-monotonic behavior due to a mismatch of the profiles of bootstrap and control current densities.

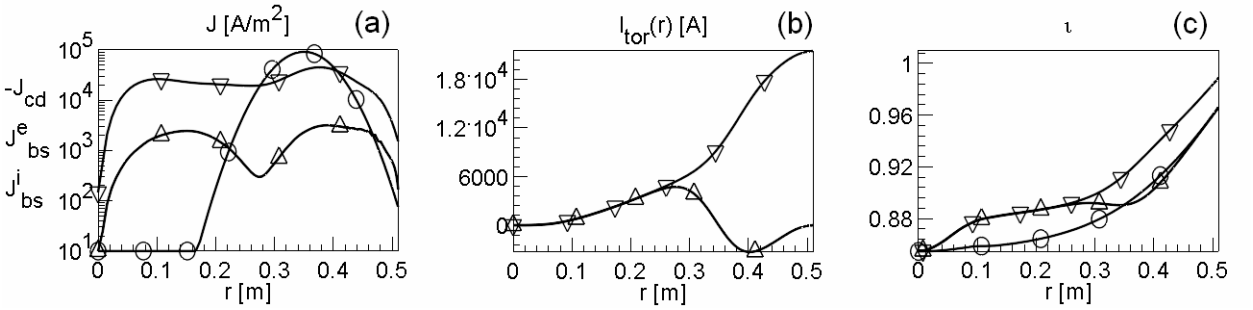


**Fig. 10**. The final current distributions and associated rotational transforms: (a) electron (∇), ion (Δ) bootstrap current densities, ECCD (O) density; (b) bootstrap (∇) and total (Δ) toroidal current distributions; (c) uncompensated (∇), final (Δ), and current-free (O) rotational transform.

Fig. 11 shows results of the simulation with the same initial conditions, but with the original 7kA of bootstrap current left uncompensated; in other words, before simulation we equilibrate the system to steady state with **P1**=0.25MW and **P2=**1.68MW, but without counter-ECCD. Then at time zero we switch on counter-ECCD produced by **P2** and start the modeling using one second reaction time in the current control algorithm. During the first 60 sec, the total toroidal current decreases slowly with the *L/R*-time of about 10 seconds, and then it behaves the same as in the case shown in Fig. 9d. Initially, the edge rotational transform $\iota_a$ has a slightly higher value compared to that of the current-free one. But it soon approaches the current-free value due to compensation of the bootstrap current.

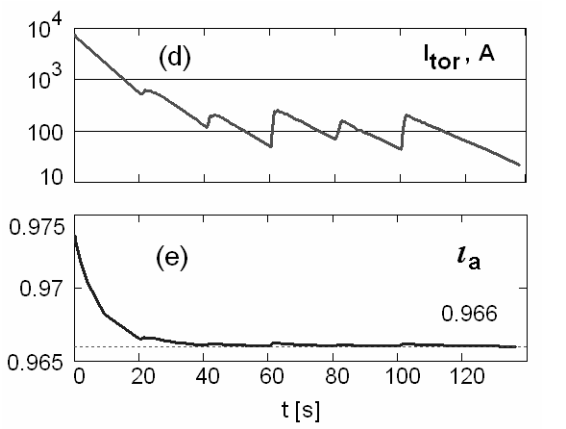


**Fig. 11**. Time traces for the case with the original 7kA of uncompensated bootstrap current: (d) the plasma current, (e) the value of $\iota_a$. The reaction time is 1 sec.

## SUMMARY

In this paper we have studied the compensation of the residual bootstrap current in W7-X by means of ECCD. The modeling has shown that sudden introduction of the counter current driven by ECRH does not instantly compensate the bootstrap current. The loop voltage induced by ECCD leads to a redistribution of the current density with a time constant of about two seconds. The relaxation time of the total current is much longer than this time – for a typical ECRH-plasma the total toroidal current reaches steady state after several *L/R*-times requiring on the order of one hundred seconds. The

simulation showed also that a strong localization of ECCD (or bootstrap current localization caused by peaked plasma profiles) leads to strong deformations of the rotational transform profile. Moreover, on-axis counter ECCD decreases the rotational transform in the central region of the plasma to zero (see also Ref. 6). In order to avoid long relaxation times and to keep the toroidal current and its profile in the acceptable range we have proposed *feed-forward* or *predictive control* methods by using ECCD as actuator. The first results of modeling have shown that it is possible to keep the plasma current within a tolerable range and also to maintain low-shear conditions for the rotational transform. The usage of ECCD and/or NBCD provides a flexible tool to control the current profile and to compensate the residual bootstrap current. It should be noted that NBCD will be available only for ten seconds during the early stage of W7-X operation[8], i.e. during a period much shorter than the relaxation time of the current. Thus, the only tool to control the bootstrap current during the initial stage of the experimental campaign will be the ECCD induced by electron cyclotron heating, which has been designed to work for 30 minutes[8]. We are planning to continue the study of *feed-forward control* schemes with the self-consistent calculation of heating and current drive included.

## REFERENCES


1. C. D. BEIDLER et al., "Physics and Engineering Design for Wendelstein VII-X," *Fusion Technology*, **17,** 148(1990)
2. Y. FENG et al., "Impact of Island Geometry on Island Divertor Performance," *Proc. 30th EPS Conf. On Contr. Fusion and Plasma Phys.*, St Petersburg, Russia, July 7-11, 2003, ECA Vol. 27A, O-4.4C
3. W.I. VAN RIJ and S.P. HIRSHMAN, "Variational bounds for transport coefficients in three-dimensional toroidal plasmas," *Phys. Fluids* B **1,** 563(1989).
4. C.D. BEIDLER et al., "Neoclassical Transport in Stellarators - Results From an International Collaboration," *Proc. 30th EPS Conf. on Contr. Fusion and Plasma Phys.,* St Petersburg, Russia, July 7-11, 2003, ECA Vol. 27A, P-3.2
5. P.I. STRAND and W.A. HOULBERG, "Magnetic flux evolution in highly shaped plasmas," *Physics of Plasmas*, **8**, 2782(2001)
6. J. GEIGER et al., "Equilibrium calculations for the W7-AS stellarator with large internal current densities due to ECCD," *Proc. 31st EPS Conf. on Plasma Phys.*, London, Great Britain, June 28 - July 2 , 2004, 2004, ECA Vol.28G, P1-207.
7. M. ROMÉ, V. ERCKMANN et al., "Electron cyclotron resonance heating and current drive in the W7-X stellarator," *Plasma Phys. Control. Fusion*, **40,** 511(1998).
8. M. WANNER et al., "Status of WENDELSTEIN 7-X construction," *Nuclear Fusion*, **43,** 416(2003)